

## Chapter 2 - Alfvén Wave Experiments

2.1	Introduction	2.1
2.2	Theory	2.2
2.3	Experimental Apparatus	2.5
2.4	Diagnostic Equipment	2.10
2.5	Experimental Conditions	2.11
2.6	Wave Velocity	2.15
2.7	Wave Attenuation	2.18
2.8	Conclusions	2.20

---

## 2.1 Introduction

The present interest in hydromagnetic waves was initiated by Alfven (1942) who considered theoretically the case of propagation parallel to a static magnetic magnetic field for frequencies  $\omega < \Omega_i$  the ion-cyclotron frequency. He suggested that waves of this type might account for some features of sunspots. This theory was extended by Aström (1950), and by many other authors in recent years.

Experimentally, the waves were first observed by Lundquist (1949) and Lehnert (1954) in liquid metals and by Bostik and Levine (1952) in a toroidal helium plasma. As the conductivity of liquid metals is comparatively low, the consequent wave attenuation introduced considerable experimental difficulties in observing waves, and most subsequent work has been carried out in gaseous plasmas. Excitation and propagation of hydromagnetic waves have been reported by Allen et al. (1959) and later by De Silva (1961) and Spillman (1963) at Berkeley. Jephcott (1959) and Jephcott and Stocker (1962) in the U.K. have measured the dispersion and attenuation of the left-hand polarized wave (see chapter 1) up to the ion-cyclotron frequency. Their results were in good agreement with the theory of Woods (1962). This mode of propagation in air plasmas has also been investigated by Nagao and Sato (1960) in Japan. More recently, a considerable amount of work has been carried out in shock produced plasmas by Brown (1966), Cross and Lehane (1968) and others. Their experimental apparatus is similar to that described in this chapter and is similar in many aspects to that described by De Silva.

Most of these experiments were carried out in cylindrical geometry on the mode of propagation which exhibits a resonance at the ion-cyclotron frequency. At frequencies below  $\Omega_i$  in the plane wave case, the wave fields exhibit torsional characteristics, with the electric vector rotating as a left-hand screw. As this is the same direction of rotation as the ions about the magnetic lines, this mode will experience collisionless damping at  $\Omega_i$ . The wave fields are considerably modified in a cylindrical plasma, but the name 'torsional wave' is still used.

In the preliminary experiments reported in this chapter, the torsional waves are generated in a hydrogenous plasma in a manner described by Furth (1959). A brief description of the theory is given below and the results of experiments in which the wave velocity and attenuation are measured as a function of frequency are shown to be in reasonable agreement with theory (Brown (1966)).

## 2.2 Theory

The 'generalized Ohms law' (Spitzer (1962)) is used with the equation of motion for the charged particles under the following assumptions.

1. Cold plasma, which implies ion and electron pressure gradients can be neglected.
2. Gravitational potential terms are neglected.
3. Electron inertia is neglected, i.e. the term  $\frac{m_e}{ne^2} \frac{\partial \underline{j}}{\partial t}$  is dropped from Ohms law.

4. Terms of order  $\left(\frac{m_e}{m_i}\right)^{1/2}$  and  $\frac{\omega}{\omega_e}$  are neglected.
5. The perturbing fields  $|\underline{b}| \ll |\underline{B}_0|$ , the applied D.C. magnetic field.
6. The wave velocity  $v \ll c$ , the velocity of light and we can consequently neglect the displacement current.

Assumption 5 means that terms only to the first order in small quantities are retained.

We then have:

$$\text{Equation of motion } \rho_i \frac{\partial \underline{v}_i}{\partial t} = \underline{j} \times \underline{B}_0$$

$$\text{Ohms law } \underline{E} + \underline{v}_i \times \underline{B}_0 = \frac{1}{n_i e} \underline{j} \times \underline{B}_0 + \underline{\eta} \cdot \underline{j},$$

and Maxwell's equations:

$$\underline{\nabla} \times \underline{E} = - \frac{\partial \underline{b}}{\partial t},$$

$$\underline{\nabla} \times \underline{b} = \mu_0 \underline{j},$$

where  $\rho_i$  is the complex mass density (due to ion-neutral collisions)

$\underline{v}_i$  is the ion velocity,

$\underline{j}$  is the current density,

$\underline{E}$  is the wave electric field intensity,

$\underline{\eta}$  is the resistivity tensor,

and  $e$ ,  $n$ , and  $\mu_0$  are the electronic charge, the charged particle number density, and the permeability of free space.

A cylindrical plasma is assumed and the perturbing quantities are assumed to vary as  $f(r) \exp i(\omega t - m\theta - kz)$  where  $m$  is the azimuthal mode number, and  $k = \frac{2\pi}{\lambda}$  is the wave number. To be able to solve this set of equations for a cylindrical plasma, the boundary conditions on the electric and magnetic fields at the plasma boundary must be considered.

For a plasma confined within a vessel with perfectly conducting walls, the tangential electric fields must vanish at the walls. For a uniform resistive plasma this case has been solved by Brown (1966) who also takes account of other radial wave modes which are launched by the simple electrode geometry.

When the plasma is bounded by a rigid non-conductor, the problem is considerably more complicated and is more fully discussed in chapter 3. By simply assuming continuity of  $b_r$ ,  $b_z$ ,  $E_\theta$ ,  $E_z$ , and of the slope of  $E_\theta$  across the non-conducting interface for a uniform plasma: (Stix (1962))

$$\frac{\gamma r J'_m(\gamma r)}{J_m(\gamma r)} = \frac{kr K'_m(kr)}{K_m(kr)}$$

where  $r$  is the radius of the plasma,  $\gamma$  is the 'radial wave number', and  $J$  and  $K$  follow the usual notation for Bessel functions (Watson (1922)).

This relation is obtained by matching the fields obtained within the plasma to the vacuum fields, which are determined by solving Maxwell's equation in free space yielding a dependence on  $K_m(\gamma r)$ , the modified Bessel function of the second kind.

For a uniform plasma density, the wave solutions are relatively simple combinations of Bessel functions. Non-uniform density gradients

require the wave equation to be numerically integrated across the radius of the plasma. The theory for a uniform plasma has been undertaken by Stix and also by Woods and others, for the case of the left and right-hand polarized waves for frequencies up to the ion-cyclotron frequency.

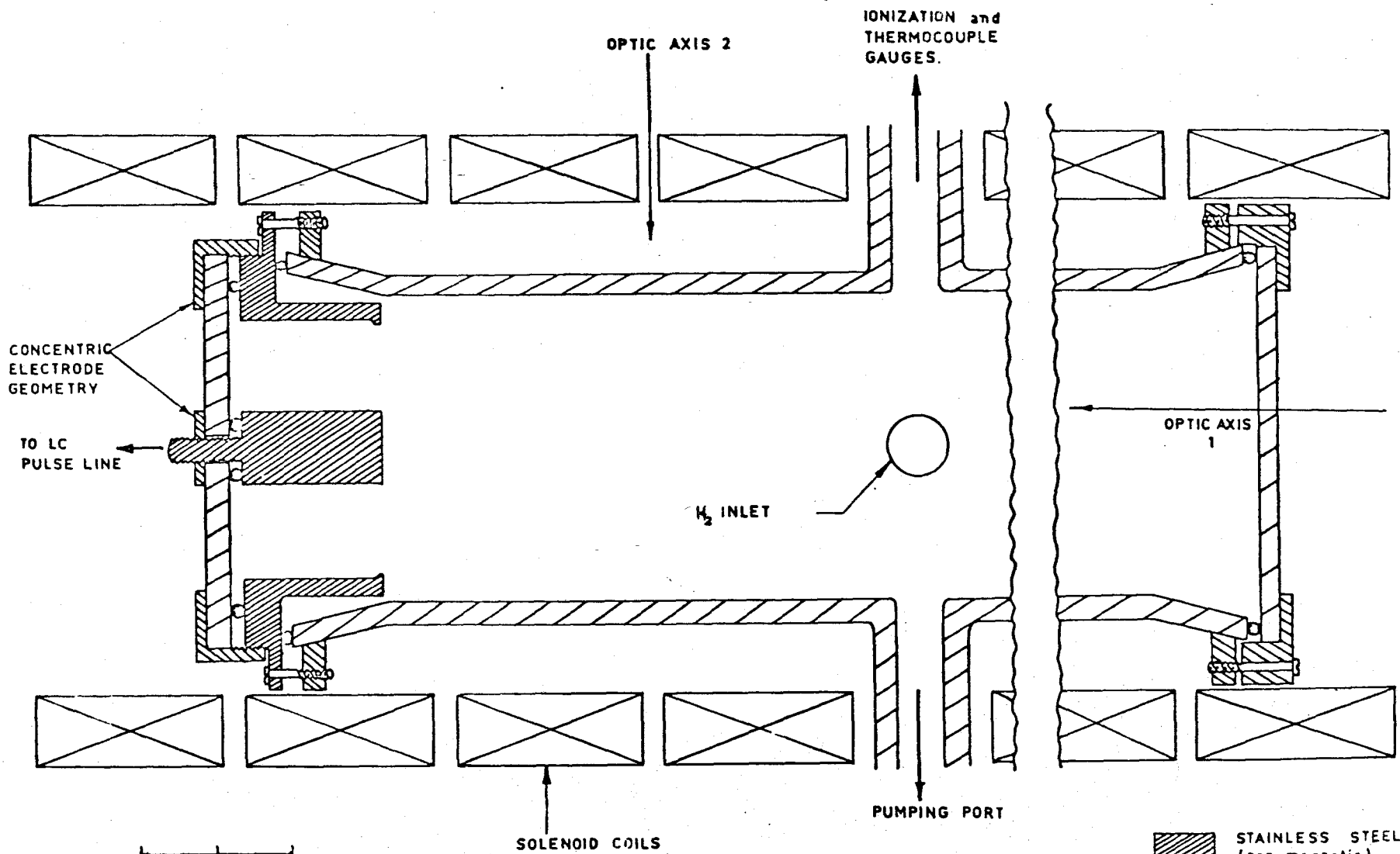
Recently, Davies (1969) has suggested that the interference of the various radial modes launched by a simple device (see, for example, Brown (1966)) will be significant when the plasma is resistive and non-uniform. He infers that this interference causes the wavefront to travel at the local Alfvén velocity near the launcher, as observed by Cross and Lehane (1968), the motion gradually changing to only the least damped mode. After the wave has travelled several wavelengths from the launching device, this least damped mode travels at a velocity which is independent of density and therefore independent of the radius.

Although the experiments described in this chapter are preliminary in nature, and only intended to demonstrate the feasibility of propagating the torsional mode, the velocity and attenuation show reasonable agreement with the results of other authors.

### 2.3 Experimental Apparatus

The wave experiments were carried out in an electromagnetic shock tube, operated with constant drive current. It is similar in design to the device used by Wilcox et al. (1962) and to the SUPPER machines of the Sydney group (Brennan et al. (1963)). The mechanical design of the present shock tube has been described by Blackburn (1970). A schematic diagram of the shock tube is shown in figure 2.1.

Fig. 2.1 Schematic diagram of the electromagnetic shock tube.



Basically, the shock tube consists of a pyrex glass vacuum vessel of inside diameter 10 cm, and length 90 cm. The vessel is situated in a 120 cm long solenoid which gives an axial magnetic field of up to approximately 8 kilogauss. A concentric electrode system is used in the glass vessel and a high radial electric field between these electrodes initiates the discharge of the shock tube.

The electrodes which are situated at one end of the vacuum vessel are made of a non-magnetic grade of stainless steel, with the outside diameter of the inner electrode being 2 cm and the inside diameter of the outer being 8 cm, leaving a 3 cm spacing. The axial length of the electrode system is 2.5 cm.

The vacuum vessel is sealed at each end by pyrex glass end plates, and has four radial ports available for access to the vessel at one axial position (20 cms from the 'firing' end). One of the ports of 5 cm diameter is used to evacuate the vessel, while another 5 cm port is connected to an Edwards ionization gauge and a Pirani gauge. The remaining two ports are of 1 cm diameter, one being used to admit hydrogen to the vessel, while the other port can be used for diagnostic purposes.

The system is evacuated by means of a 2 inch oil diffusion pump, backed by a two-stage mechanical pump. No trapping of any kind is employed and this limits the base pressure attainable in the vacuum vessel to about  $2 \times 10^{-6}$  torr. As the device was operated with gas pressures in the range 30 - 300 millitorr, this base pressure was quite sufficient to maintain a low impurity level. The period between operation of the machine was sufficient to allow complete replacements of the test gas, together with any attendant impurities released by the current flow in the shock.

Hydrogen, the only gas used in the investigations, is admitted continuously to the vessel after being purified by diffusion through a heated palladium thimble. Gas pressure can be varied by a combined manipulation of the baffle valve, to vary the pumping speed of the diffusion pump, and the flow speed of the incoming gas. The hydrogen pressure in the vessel was monitored continuously by the Pirani pressure gauge.

The vacuum vessel is surrounded by a solenoid which, when energised, supplies an axial magnetic field of up to 8.1 kilogauss uniform to within  $\pm 3\%$  over the volume occupied by the plasma. Because of the sudden movement of the solenoid when it is energised, the vacuum vessel is not attached to the solenoid, but is free to move within it, so that any movement is not transmitted to the vacuum vessel. The energy source used was a capacitor bank of total capacity 6 millifarad which could be charged to 2700 volts. The maximum on-axis variation is  $\pm 2\%$  at an average field of 5.1 gauss/amp.

When the capacitor bank was discharged, the maximum current through the solenoid was 1.6 kiloamps. The total inductance of the solenoid was 8.9 millihenry which gave a risetime for the magnetic field of 10.5 milliseconds.

The plasma was formed by the passage of a normal ionizing shock wave driven by the axial  $\underline{j} \times \underline{B}$  force acting on the current sheet behind the shock wave. For constant shock velocity and steady shock behaviour, the current should be constant at the required level for a period at least as long as the time needed for the shock wave to traverse the length of the shock tube. The bank of capacitors used consists of

six 8.5 uF, 20 kV capacitors connected in the form of an artificial transmission line, of characteristic impedance approximately 0.5 ohms. Inductors of 6 turns of 3/16" copper tube wound on a 2½" former were found to give a current pulse with the required length and risetime. The maximum current is 40 kiloamps, constant for 40 μ seconds and with a risetime of 6 μ seconds.

The capacitor bank is discharged when the axial magnetic field is at its peak value by firing a type BK 178 ignitron. The current flows to the shock tube through six parallel high-voltage coaxial cables. A variable stainless steel resistor in series with the discharge circuit is used to match the impedance of the source and load. A second ignitron was used to short out the current just before the shock front reached the far end of the tube, to minimize end plate ablation and stop the plasma rotating.

With a magnetic field of 8.1 kilogauss, the ion-cyclotron frequency is approximately 12 MHz. An oscillating circuit capable of producing high power in the megahertz region is then required for launching the torsional wave. A simple inductance-capacitance oscillating circuit with reasonably high Q (capable of producing some tens of cycles) was decided upon. High voltage ceramic capacitors of 1000 pfd were used and could be charged up to a maximum of 15 kilovolts.

In the frequency range 0.5 to 8.0 MHz, a simple structure with up to 16 capacitors in parallel was connected to the firing electrodes of the shock tube with high-voltage coaxial cables. For higher frequency studies in the range 5.0 to 15.0 MHz a coaxial structure housing the capacitors was connected directly to the electrodes, and discharged via a spark gap.

Considerable trouble was experienced using a centre trigger electrode to discharge the capacitors. A number of different methods were tried and a trigger unit using thyatron and ignitron switching to discharge a separate capacitor through a small subsidiary spark gap was finally constructed. This spark gap was positioned two inches from the main spark gap, and provided a source of ultra-violet radiation which ionized molecules in the main gap, causing it to break down. This configuration had the advantages of a small shot to shot variation in breakdown time and the added safety of having the trigger gap physically separated from the main gap. Many experiments proved this to be the most reliable method of exciting the waves.

#### 2.4 Diagnostic Equipment

Magnetic probes were used to determine the velocity and attenuation of the wave. These were inserted into the plasma from the end opposite to the electrodes through reentrant quartz sheathing, which could be moved longitudinally through a vacuum seal. Two sizes of quartz sheaths were used, 13 mm O.D. for the initial experiments and 6 mm O.D. for later experiments requiring greater spacial resolution of the wave fields. Most probes were wound with 40 S.W.G. enamelled wire on 2 mm or 4 mm diameter formers. An earthed centre tap on the probe coil allowed the rejection of a large common signal (due to electrostatic pick up). The outputs from the two sides of the coil were taken via two coaxial cables to a Tektronix type 551 oscilloscope and added out of phase by using a type G plug-in unit. The oscilloscope was housed

in a double-shielded Faraday cage and the cables and leads to the probe coil were shielded by an earth screen joined to the outside of the cage. Photographs of similar probes are included in chapter 6.

In some experiments where the variations of the wave fields  $b_r$  and  $b_\theta$  were required simultaneously, two probe coils with their axes perpendicular were used. The effect of shot to shot variation could thereby be minimized. To determine the radial variation of the wavefront, a 'bent' probe was used. A Rogowski belt was used to monitor the current from the wave capacitors to the launching electrodes.

During the latter experiments, a polychromator (Stirling and Westwood (1968)) became available for use on the plasma. By splitting the  $H_\beta$  spectral line into seven wavelength bands, the density of the plasma could be determined immediately by Stark broadening calculations. The magnetic probes were calibrated in a parallel plate inductance connected to capacitors which were varied to "ring" at the same frequency as the wave. The geometry of the parallel plates gave a uniform magnetic field which could easily be calculated by measuring the current flowing through the plates.

## 2.5 Experimental Conditions

A prompt surface wave which travelled along the interface between the plasma and cold gas near the boundaries caused considerable difficulty in wave measurement. The prompt and Alfvén waves interfered in this region making measurements of the time of arrival of the wavefront impossible.

A number of subsidiary experiments were carried out at 2 MHz to determine the best initial gas pressure and time after breakdown to launch the waves.

High speed framing camera photographs have shown the plasma to be quite turbulent in the initial stages and it was therefore allowed to decay to a quieter state at about 140  $\mu$ s after initiation of the shock current before the Alfvén waves were launched. Two neutral gas pressures were chosen for the majority of the experiments, 57 millitorr and 130 millitorr of hydrogen. Except for measurements on the curvature of the wavefront, the magnetic probes were situated 2 cm off axis and oriented to measure the  $b_{\theta}$  component of the wave field.

To determine the best time to launch the waves without interference from the surface mode, a pressure of 130 millitorr was chosen and torsional waves launched at times varying between 140  $\mu$ s and 400  $\mu$ s after breakdown of the gas by the shock wave. These measurements showed the surface wave to be dominant after about 250  $\mu$ s at this radial position of the probe.

The onset of the surface wave was detected by a rapid change in delay time between the transmitted and received signals, and by a change in the wave amplitude. As seen from framing camera photographs, the decay of the plasma involves a decrease in the radius of the ionized centre. This brings the low ionized outer region of the plasma closer to the probe and the surface wave signal dominates the signal seen by the probe. When the probe was less than 40 cm from the electrodes, surface wave interference was detected for pressures below 50 millitorr.

As the waves are propagated within a cylinder, the right-hand or compressional wave which may also be excited with the torsional wave has a low frequency 'waveguide' cut-off (Woods (1962)). This cut-off is defined by

$$\omega_{co} = V_A \gamma$$

where  $V_A = \frac{B_0}{(4\pi\rho)^{1/2}}$  with  $\rho$  being the mass 'density' and depends on  $\omega_{in}$  the ion-neutral collision frequency.

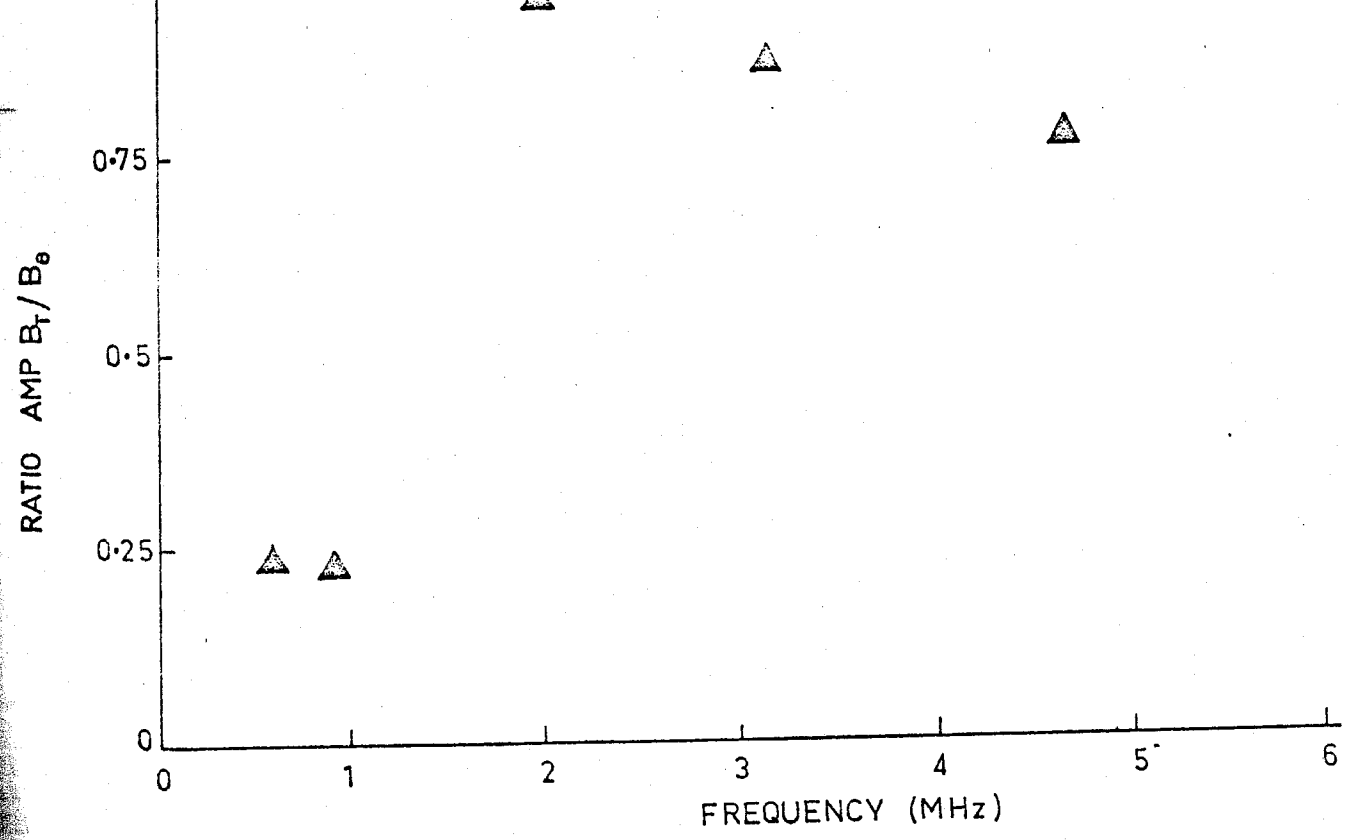
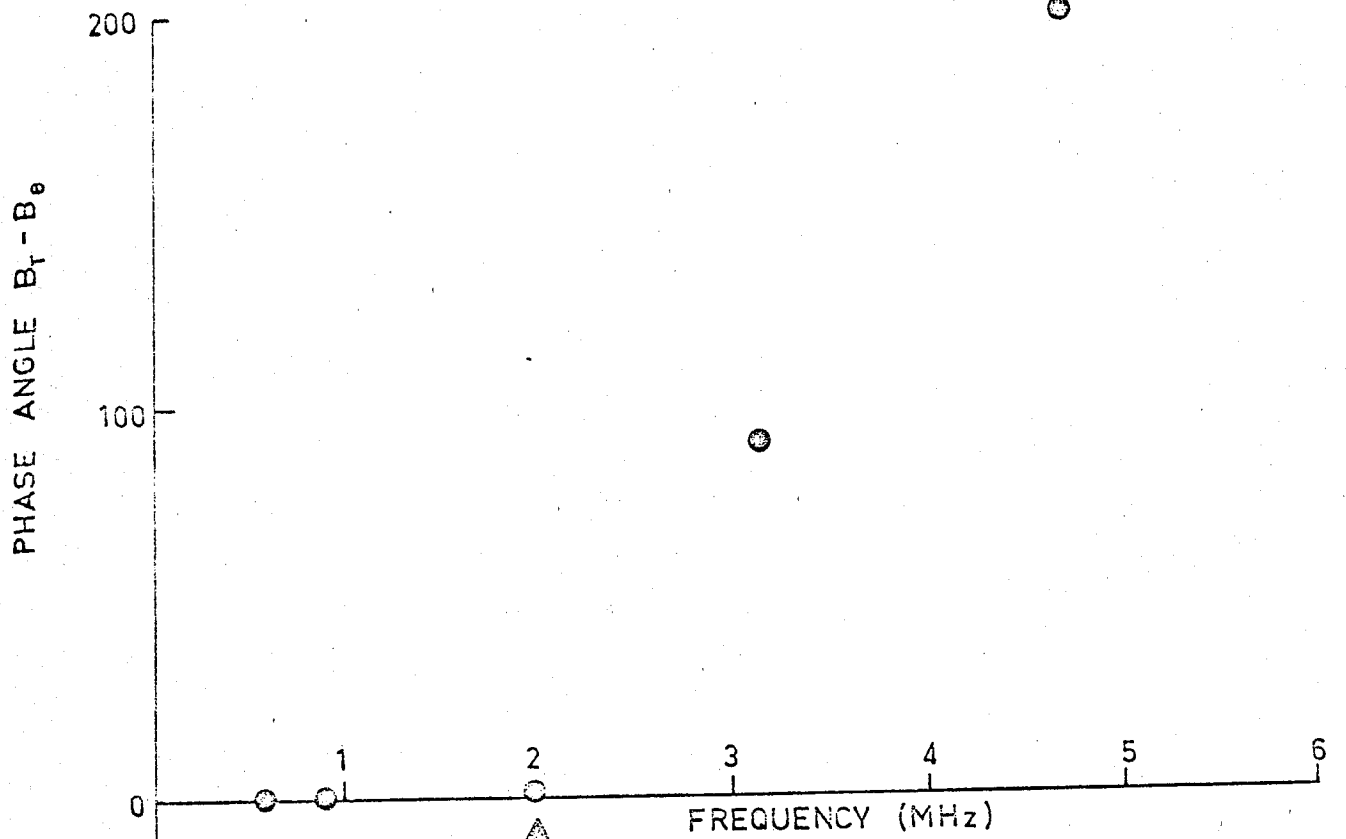
The radial wave number  $\gamma$  is defined by the boundary conditions. With an ion density of  $1 \times 10^{15}/\text{cc}$  and 8.1 kilogauss,  $\omega_{CO}$  was estimated to be in the low megahertz region, below  $\Omega_i$  the ion-cyclotron frequency.

To measure the pure torsional mode, the wave frequency must be below the cut-off frequency. At frequencies far below  $\Omega_i$ , the torsional wave field is predominantly azimuthal, while the compressional wave field is axial and radial. The cut-off frequency can in this case be determined by measuring the relative amplitudes of  $b_r$  and  $b_\theta$  and also by the change in phase between  $b_r$  and  $b_\theta$  (Spillman p.64). The experimental results are shown in figure 2.2.

To eliminate interference caused by the surface waves, a pressure of 130 millitorr and a wave time of 145  $\mu\text{s}$  were chosen with the probe 12 cm from the launching electrodes. Each point is an average over data taken from three shots using the double coil probe oriented to measure  $b_r$  and  $b_\theta$ . The transition is seen to be gradual between 2 MHz and 4 MHz, also observed by Spillman who suggests that alignment of the probe and probe proximity to the electrodes will prevent a sharp transition from being observed.

The torsional waves were launched into the plasma with a peak wave magnetic field strength  $|b_\theta| = 50$  gauss giving a perturbation ratio of  $|b_\theta|/|B_0| = 0.006$ . This allowed linearization of the wave equations for the perturbing quantities.

Fig. 2.2 Phase angle between  $b_r$  and  $b_\theta$  and ratio of the amplitudes of  $b_r$  and  $b_\theta$  as a function of frequency.



## 2.6 Wave Velocity

By measuring the difference in time from the outset of the current into the plasma, monitored by a Rogowski belt, to the signal detected by a magnetic probe immersed in the plasma, the wave velocity could be found. The delay measured by the probe signals was plotted against the axial position of the probe (figure 2.3). As the initial cycle or two were distorted and of a lower frequency than the rest of the wave train, the position of the third or fourth peak was generally plotted. This initial distortion of the wave form has also been observed by Spillman. The probe was at a radial position of 2 cm off-axis where the first radial mode of the wave aximuthal field,  $b_{\theta}$ , was expected to have a maximum. The neutral gas pressure for the velocity and attenuation measurements was decreased to 57 millitorr which increased the compressional wave cut off to above about 3MHz. The waves were launched 145  $\mu$ s after breakdown at a frequency of 2 MHz and should therefore be purely torsional.

The velocity of the surface wave was not accurately measured, but was at least an order of magnitude greater than that of the Alfvén waves. As before, the results in figure 2.3 are an average over three shots of the plasma. The average velocity for the torsional waves at a radius of 2 cm was found to be  $38 \pm 5$  cm/ $\mu$ s for a gas pressure of 57 millitorr. Spectroscopically, the ion density at 145  $\mu$ s after breakdown was approximately  $1 \times 10^{15}$ /cc. As this is an average density across a diameter of the plasma, which is certainly non-uniform, an experiment to determine the time of arrival of the wavefront as a function of the radius of the tube was carried out at one axial position and a frequency of 2 MHz. The probe was approximately 30 cm from the launching electrodes.

Fig. 2.3 Velocity determination from difference in time from onset of current into the plasma to the signal detected by a magnetic probe at different axial positions in the plasma.

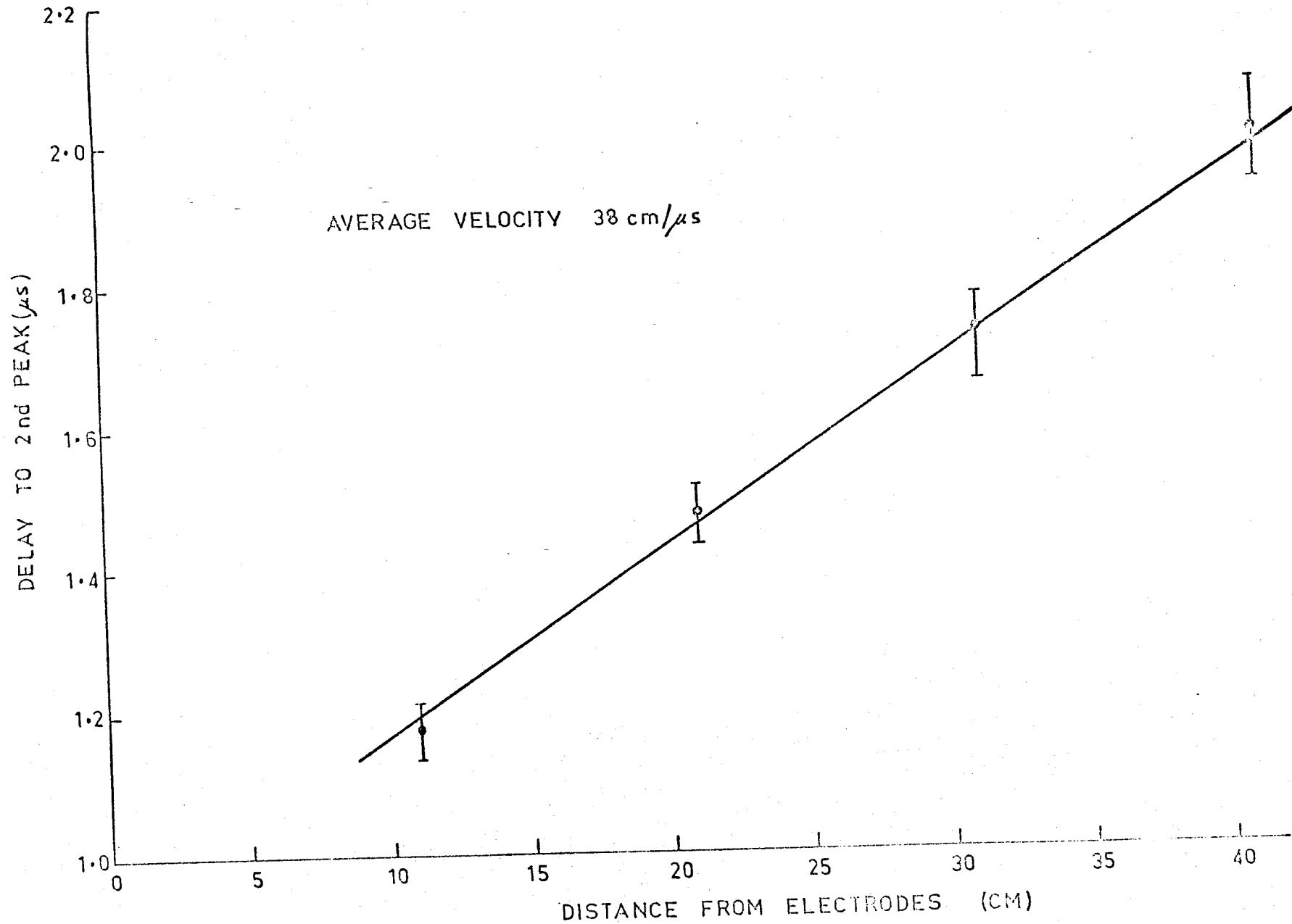
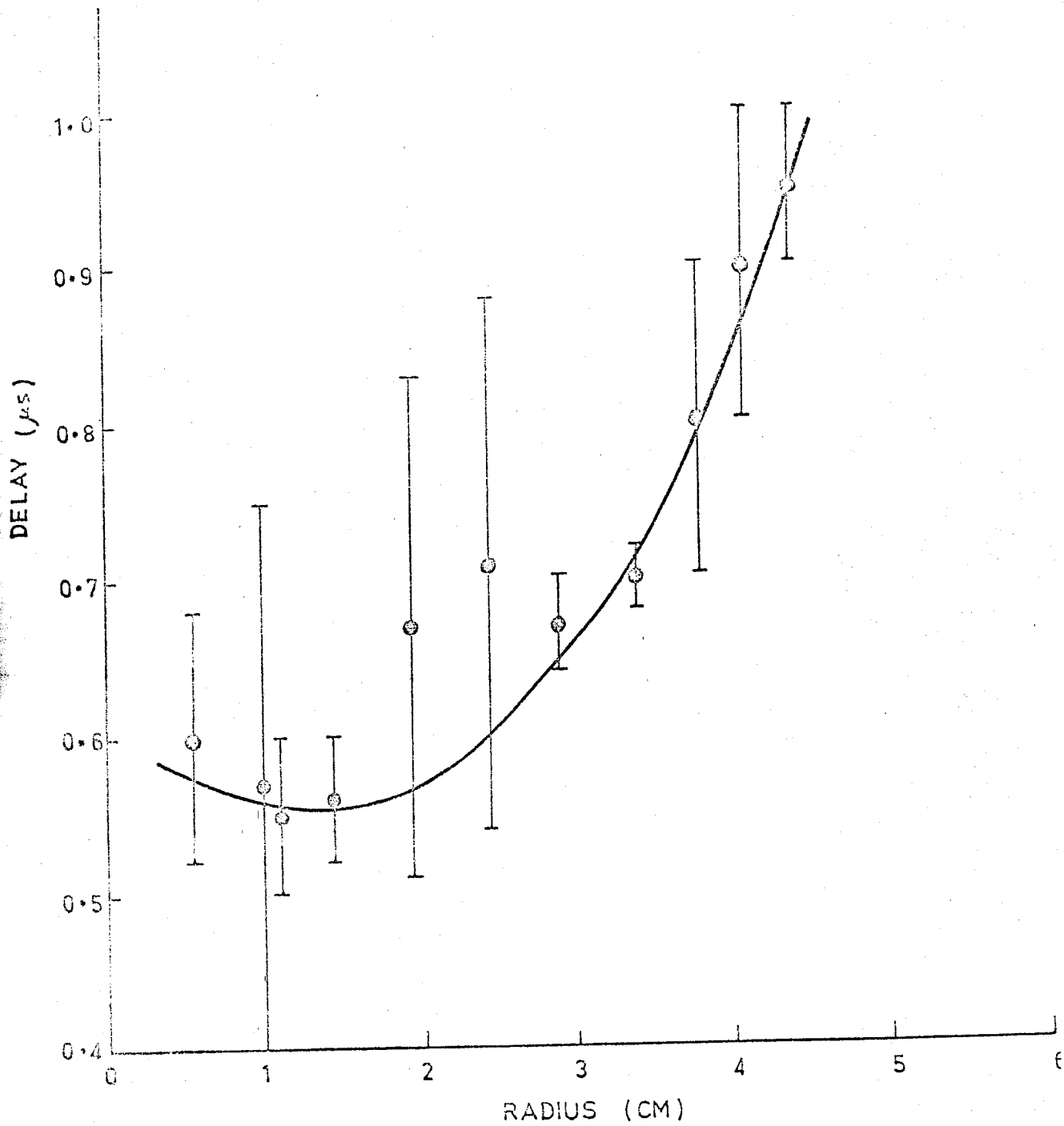


Fig. 2.4 Time of arrival of wavefront at a specific axial position as a function of radius.



The axial bent probe which could be rotated from the wall to the centre of the tube was used for this experiment. The results are illustrated in figure 2.4 and show the radial variation of arrival time.

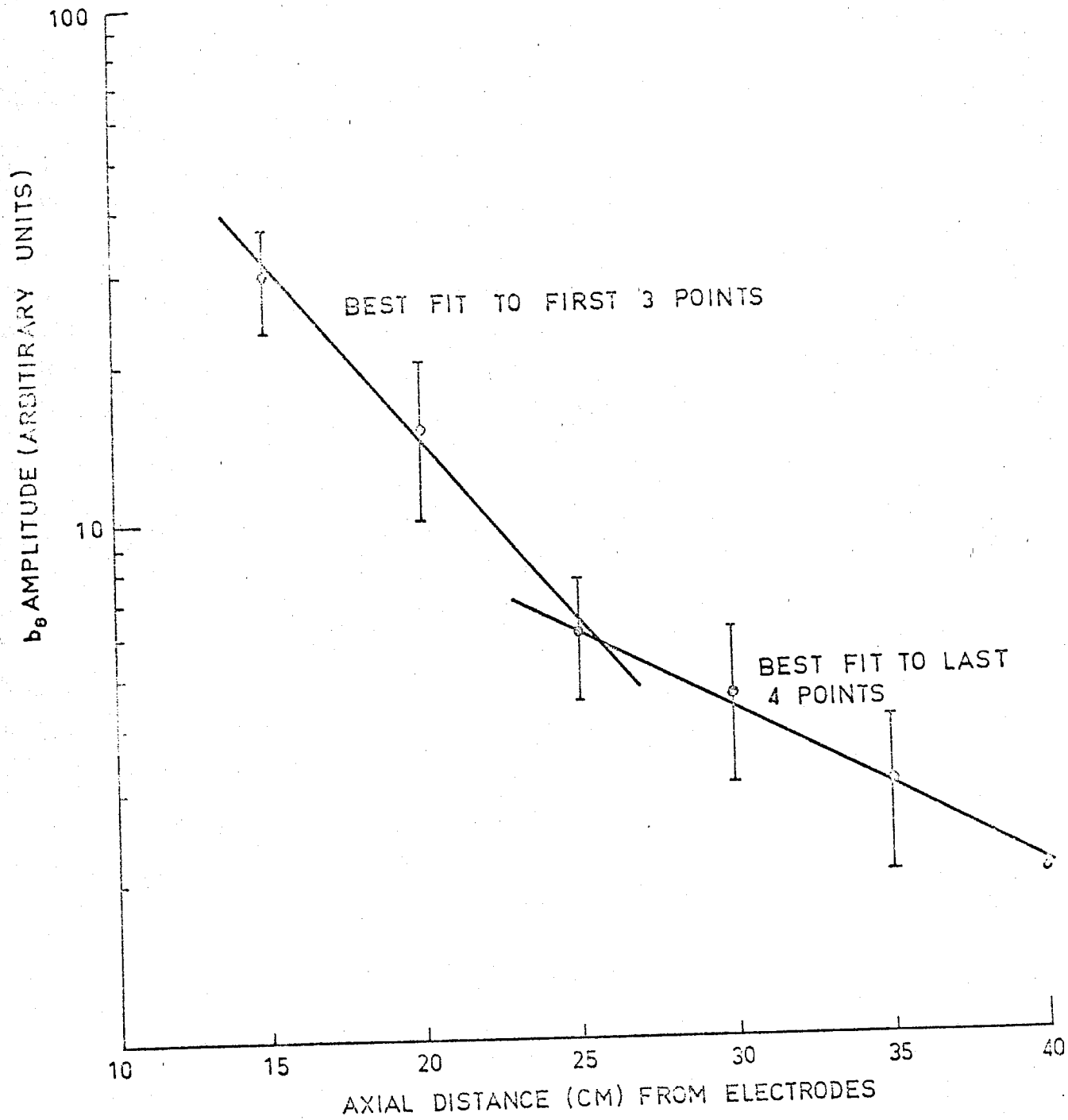
By taking measurements at different axial positions, Cross and Lehane (1968) found a velocity variation with radius, the velocity being determined by the local Alfvén velocity in the non-uniform radial density gradient. Pneumann (1965) and Davies (1969) have investigated the theoretical aspects of this problem. The present results show the same trend as those of Cross and Lehane.

## 2.7 Wave Attenuation

Since an exponential wave attenuation is expected, the measured wave amplitudes are plotted on log-linear graph paper. The line of best fit through the experimental points is used to determine the attenuation length. Figure 2.5 shows such a plot of amplitude versus axial position of the magnetic probe. As these experiments were carried out soon after the shock tube had been commissioned, accurate measurements of the ion density and temperature had not been taken. Approximate values of the parameters were:

Initial particle density	$4 \times 10^{15}/\text{cc}$
Ion density at 145 $\mu\text{s}$	$1 \times 10^{15}/\text{cc}$
Percentage ionization	30%
Temperature	1 eV
Collision cross section	$7.5 \times 10^{-15} \text{ cm}^2$ (From Brown 1966)
Neutral density at 145 $\mu\text{s}$	$2 \pm 1 \times 10^{15}/\text{cm}^3$ (See section 2.8)

Fig. 2.5 Determination of attenuation by plotting wave amplitude as a function of axial distance. Wave frequency 2.0 MHz, pressure 57 millitorr.



As can be seen from figure 2.5, the attenuation is greater closer to the electrodes which is probably due to mode mixing. The attenuation reaches a stable value at distances greater than 30 cm or approximately 1.5 wavelengths from the electrodes.

## 2.8 Conclusions

The velocity and attenuation measurements are in qualitative agreement with other authors, although phenomena such as the propagation of the surface wave and the curvature of the wavefront are not yet fully understood.

At low frequencies, the wave damping is mainly resistive due to electron ion collisions, but at higher frequencies, the effect of ion-neutral collisions must be accounted for. The ion-neutral collision frequency  $\omega_{in}$  is defined by

$$\omega_{in} = n_n \sigma_m V_i$$

where  $n_n$  is the number of neutrals,

$\sigma_m$  is the ion-neutral collision cross section for momentum transfer,

$V_i$  is the mean thermal velocity of the ions.

The value of  $\sigma_m$  deduced by Brown<sup>(1966)</sup> is  $7.5 \times 10^{-15}$  cm<sup>2</sup>, and we take an average ion temperature  $T_i$  of 1 electron volt deduced from relative line intensities of the Balmer series. At 145  $\mu$ s after breakdown and with an initial neutral gas density of  $4 \times 10^{15}$  atoms/cc, the average ion density across a diameter was  $1 \times 10^{15}$ /cc. Jephcott and Stocker (1962), and Brown (1966) have observed that a loss of particles to the

walls occur after the passage of the shock front. Hence the number of neutrals present at the wave time was estimated to be  $2 \pm 1 \times 10^{15}/\text{cc}$ . These results give a collision frequency  $\omega_{in}$  lying between 1.5 MHz and 4.5 MHz. As the waves were propagated in this frequency region, ion-neutral collisions were beginning to play an important part in the wave damping (Brown (1966)).

Since the ion-cyclotron frequency of 12 MHz is large compared with the wave frequency of approximately 2 MHz, the wave travels at the local Alfvén velocity

$$v_A = \frac{B_0}{(4\pi\rho)^{1/2}} \quad , \quad \rho = nm$$

where  $n$  is the total particle density (including neutrals) for wave frequencies  $\omega < \omega_{in}$ . A value of  $n$  of  $2 \times 10^{15}/\text{cc}$  is required to give the experimental velocity of  $4 \times 10^7$  cm/second. As the ion density was measured to be  $1 \times 10^{15}/\text{cc}$ , the neutral particles can be seen to be playing an important role in the wave dispersion. Above  $\omega_{in}$ , the neutrals became less important, their motion lagging further behind the ion motion.

Using the boundary conditions for rigid non-conducting walls for a uniform plasma derived by Stix a "theoretical" value for  $\gamma a$  of  $2.8 \pm 0.1$  is obtained (where  $\gamma$  is the radial wave number, and  $a$  is the plasma radius). By using the measured value of the cut-off frequency for the compressional wave (figure 2.2), and assuming the plasma radius to be the same as the radius of the vacuum vessel, the experimental value for  $\gamma a$  is  $2.1 \pm 1.0$  comparing well with the theoretical value above.

These preliminary results showed that it was possible to launch torsional Alfvén waves into the shock produced plasma provided care was taken to keep the wave frequency below  $\omega_{co}$ , and the plasma parameters adjusted to eliminate interference from the surface wave from the region of investigation. As the original intention was to investigate collisionless damping of the torsional wave at the ion-cyclotron frequency, this frequency  $\Omega_i$  must be lower than the waveguide cut-off for the compressional wave. The relations for these two frequencies are:

$$\omega_{co} = \frac{B_0 \gamma}{\sqrt{4\pi\rho}} \quad , \quad \Omega_i = \frac{eB}{m_i} .$$

Since the ion-cyclotron frequency is independent of the particle mass density  $\rho$ , if this was lowered,  $\omega_{co}$  could be made greater than  $\Omega_i$ .

Ion-cyclotron wave studies at Princeton use a plasma density of approximately  $10^{13}$  ions/cc, which would make the cut-off frequency a factor of two higher than the cyclotron frequency. With the plasma described in this chapter, this could be achieved by launching the waves in the afterglow of the plasma. However, the plasma radius decreased with time after breakdown and the wave signal was swamped by the surface wave. The degree of ionization, and consequently, the conductivity had also dropped with the consequence of prohibitively high attenuation of the waves.

Attempts to lower the plasma density by decreasing the gas pressure were equally unsatisfactory. The shot to shot variation in plasma conditions produced by launching the shock front with gas pressures below 40 millitorr, increased to greater than a factor of two until at pressures

below 15 millitorr, the applied voltage was not sufficient to cause breakdown of the gas at the electrodes.

It was obvious that a low density, highly ionized plasma with a small shot to shot variation was needed to study the propagation of small amplitude waves in the region of the ion-cyclotron frequency. The following chapters of this thesis present a theoretical and experimental investigation of plasma production using a standing helicon wave 'resonance' in an argon plasma. The density and degree of ionization of the plasma so formed makes possible the study of the collisionless damping mechanism mentioned above.